Expansion characteristics and invasion in hot rarefied expanding plasma flows

O. Gabriel, P. Colsters, R. Engeln, D.C. Schram

Technische Universiteit Eindhoven, P.O. Box 513, 5600 MB Eindhoven, The Netherlands

Abstract. In this presentation the expansion of hot plasma in a low pressure background is investigated in detail by laser induced fluorescence on argon metastables. Detailed velocity distributions reveal that there are two distributions: a fast, cool supersonic expanding one and a slow, warm component resulting from invasion. It is found that the invading component is first present at the outside of the barrel shock and that it gradually migrates inward. The supersonic component, which of course first dominates, shows all characteristics of rarefied shocks: acceleration to two times the source acoustic speed, adiabatic cooling, and a parallel temperature, which remains higher than the perpendicular.

INTRODUCTION

The expansion of hot fast flowing plasma and gas has received attention from several backgrounds ranging from large astrophysical objects to minute size laser spots. The use of expansion for high rate plasma processing is more recent. Accurate analysis by several diagnostic techniques, which take advantage of the plasma nature, in the presence of electrons, excited and radiating particles has given new possibilities to analyze the nature of expansion. The use of plasma with its high temperatures brings the expansion to an interesting rarefied regime as pointed out earlier by Campargue [1]. Then efficient plasma sources are to be combined with high pumping speed and short residence times [2]. It is the purpose of this paper to add new spatially resolved information on velocities and temperatures in rarefied expansion by the use of LIF on argon meta-stables. In gas expansion experiments with electron beam fluorescence it was found by Muntz et al. [3] that two distributions exist: a supersonic and a subsonic one. These were explained as a gradual transition from supersonic to subsonic flow as described by Mott-Smith [4].

In earlier studies with TALIF [5] on atomic hydrogen it was shown that two effects are present in the expansion of mixtures, both were already identified earlier by Campargue: the mass focusing effect in the early expansion and invasion in the later phase of the shock, the over-expanded region [6]. Mass focusing is caused by the difference in expansion velocity of lighter and heavier components and subsequent scattering out of the lighter particles. Invasion gives the reverse effect: in rarefied conditions the lighter particles are preferentially scattered in the supersonic expanding beam. Invasion is also present in a one component expansion: it creates, besides the fast cool supersonic plasma component, a slow hotter component, which results from scattering between the supersonic particles and invading particles from outside the barrel shock [7]. This effect can become very important if the shock becomes rarefied, i.e. if the mean free path becomes comparable with the gradient length, the shock size.

For plasma chemistry the appearance of this invasion is important as it facilitates the inflow of molecules from the outside and therewith alleviates the mixing of molecules with the hot plasma beam from the source. In that field also detailed information has been obtained from various techniques as Thomson and Rayleigh scattering [8][9], two photon laser induced fluorescence [10] and LIF on meta-stables [7]. These give values for electron and neutral densities and temperatures, on densities, temperatures and velocities of atomic radicals and of metastable atoms.

We will first describe the expansion and give details of earlier measurements on argon expansions. Then we will compare these results with the outcome of the Bird code [11], a direct simulation Monte Carlo code. We will do so for conditions which are relevant for fast plasma processing. One example is the fast deposition of amorphous or nano crystalline layers for solar cells with silane injected in an argon/hydrogen plasma beam.

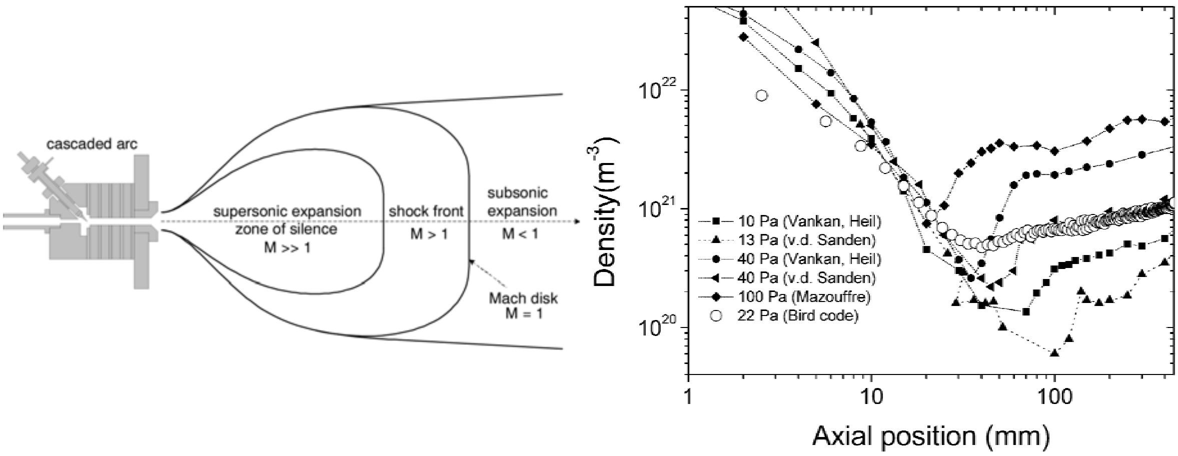

Figure . *Left:* Expanding plasma from cascade arc source with supersonic part, shock front and subsonic expansion.
Right: Axial evolution of neutral density measured with Rayleigh scattering in our group compared with Bird code simulation.

DESCRIPTION OF EXPANSION AND MEASUREMENTS

The plasma expands from a thermal plasma at sub-atmospheric pressure, see figure 1. The cascade arc has a bore of $2a_0 = 4$ mm through which an argon flow of $\hat{\Phi} = 50$ sccs and a current of 45 A flows. In the arc the temperature of electrons and of neutrals and ions is approximately 1 eV, decreasing to an exit temperature of 0.6 eV, an exit pressure of $3{\cdot}10^4$ Pa and a sonic exit velocity of $c_0 = 1550$ m/s [7].

The exit pressure can be related to the flow according to $\Phi = p_{exit}\, \pi\, a_0^2\, c_0 / kT$. After exiting the arc source the plasma starts to expand and the density decreases quadratically with distance z to the source: $n(z) = n_0 / (1+z_0^2/z^2)$. Here z_0 is roughly the radius of the arc column, a_0.

From the momentum balance the velocity evolution can be deduced: it increases over a distance of a few arc diameters to two times the exit velocity $2c_0$: $w_z^{\infty} = 2c_0$.

The temperature decays adiabatically; at these low densities even for atoms and molecules as there is no time for conversion and all particles are frozen in. The plasma expands and cools and after a distance of ½ z_M, halfway the position of the Mach disk at $z = z_M$ it over-expands and forms a valley: the density becomes lower than the background density. When the stagnation pressure approaches the background pressure the plasma passes a shock front, after which subsonic expansion follows. If before the shock the Mach number M >> 1, then the density increases a factor 4, whereas the velocity decreases a factor 4. The temperature increases to a value close to that at the source [12]. Its value is determined by the energy input from the source and loss by heat conduction. [13].

In figure 1 the density evolution, measured with Rayleigh scattering, is shown for the conditions mentioned above and for various pressures. The various characteristics of the expansion are evident: the initial density n_0, the z_0^2/z^2 decrease, the valley starting at ½ z_M, the diffuse shock front at z_M and the subsonic expansion, in which the density increases because the temperature decreases. The position of the shock front is indicated by z_M; it decreases with increasing pressure. In this figure also the results of DSMC calculations are given (Bird) for two pressures (20 & 100 Pa). It shows that the code describes the expansion satisfactory. Only the density depression is less developed, probably because of the used hard sphere approximation for the neutral-neutral collisions.

The position of the shock front z_M is predicted at ($\hat{\Phi}$ in sccs, $\hat{T}_s$ in eV) [14]

$$z_M = C \cdot 2a_0 \sqrt{\frac{p_{exit}}{p_{back}}} = 0.02 \sqrt{\frac{\hat{\Phi}}{p_{back}} \sqrt{\hat{T}_s A}} \ \text{[m]}$$

It scales according to predictions with the square root of 1/ p_{back}. At the lowest pressures, the mean free path for argon atom-atom collisions becomes of the same order as ½z_M and thus the flow becomes rarefied. This regime is thus easier reached with hot plasma. To analyze the situation further velocity distributions are measured by LIF on the argon 1s5 meta-stable. An earlier result [7] giving velocity and temperature shows clearly the acceleration to $2c_0$;

but also the appearance of a second distribution of scattered in particles was visible. On one position at z= 50 mm in the valley a radial scan was made. From this scan it was clear that the second distribution, the scattered in one, became more important for off centre positions. It is the purpose of this contribution to analyze the spatial distribution in the barrel shock of the two components. We will first shortly summarize the measurement technique.

DETAILED MEASUREMENTS OF VELOCITY AND TEMPERATURE WITH LIF

A small bandwidth diode laser with λ = 772.6 nm is used to excite the argon metastable in the 1s5-2p7 transition. The fluorescence is observed perpendicularly to the diode laser beam, which is either directed parallel (||) or perpendicular ($\perp$) to the axis along the expansion direction. The laser is scanned stepwise with 2000 points/nm; the fluorescence signal is detected with a photo multiplier and is integrated with an integration time of 0.1 – 2 s. Deviations from wavelength linearity are corrected with help of a Fabry Pérot interferometer.

If the laser is directed parallel to the z-axis the parallel component of the velocity distribution is measured and thus the axial component of the average velocity and the parallel temperature, $T_{\|}$. Likewise perpendicular irradiation yields the perpendicular velocity distribution and thus the perpendicular component of the velocity and $T_{\perp}$. It will appear later that in the supersonic expansion there is difference between $T_{\perp}$ and $T_{\|}$.

Metastable atoms are produced in this expanding plasma by three particle recombination of Ar^+ ions and electrons. The resulting high excited states are de-excited by electrons and cascade further to the 4s metastable (1s5, 1s3) or resonant (1s4, 1s2) levels. At high electron densities these levels are coupled [15] and the main loss is by trapped resonant line radiation. In our case H_2 is admixed and thus the electron density is effectively destructed by molecular assisted recombination [16]. This is purposely done to reduce the metastable density and therefore to avoid absorption of the laser signal. Actually a finite absorption was still present for the first points of the expansion (which gives a value of the absolute density). However what is of interest here is not the density, but the velocity distribution and the appearance of an additional component besides the supersonic one further down in the expansion. We are interested in the behavior of the neutrals and the question is in how far the metastables reflect that of the neutrals.

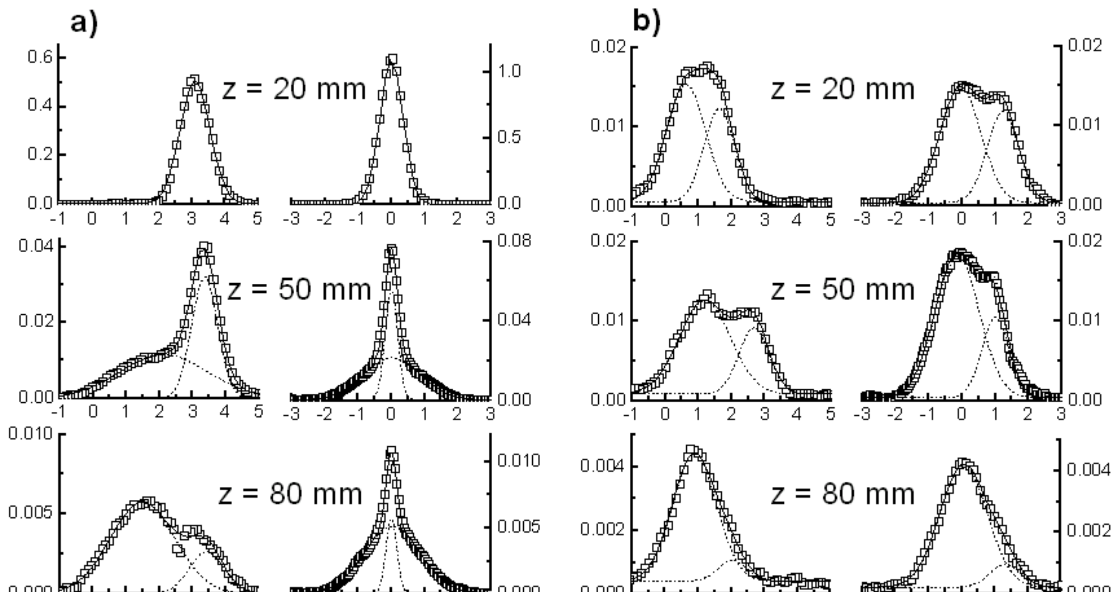

Figure 2. Measured axial and radial velocity profiles, each fitted with two Gaussian profiles at three different z position: a) at the center line (r = 0 mm) and b) at r = 20 mm.

The metastables are formed from ions and have therefore in first instance the ion distribution. During their lifetime they collide elastically (and by resonant excitation exchange) with argon neutrals, after a short distance from the source by far the most abundant particle. The mean free path for m0 collisions, λ^{m0}_{mfp} is much smaller than the corresponding one for 00 collisions, λ^{00}_{mfp}. The latter becomes at the point of smallest density of the same order as the gradient length, so the shock becomes rarefied. The metastables are however by their much larger cross section tightly coupled to the neutrals; the λ^{m0}_{mfp} is much smaller than the gradient length and thus their distribution closely reflects that of the neutrals.

During the first phase of the expansion the metastables, born with ion distribution, are depopulated by electron induced coupling with the resonant states and radiation loss by trapped resonance radiation [15]. But further away the electron density becomes small and coupling by heavy particle collisions is slow; Thus here the loss is by convection. This can be concluded readily from the z-dependence of the metastable density n_m, which shows the typical expansion behavior of $1/z^2$ [7]. In the subsonic regime gradient lengths become large and again the metastable density is locally determined by production and loss processes.

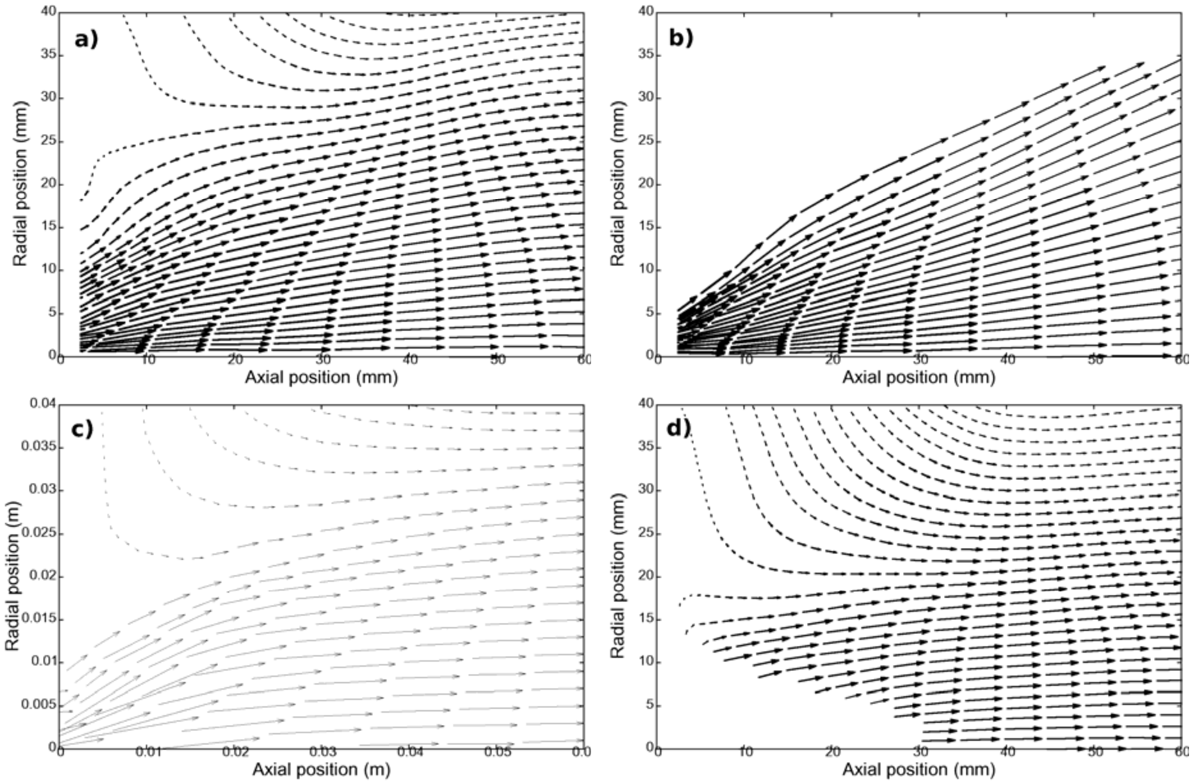

Figure 3. Measured flow pattern based on interpolated axial and radial velocities (arrow direction and length) and densities (arrow thickness). a) Mean measured velocity, b) expanding component only, d) scattered component only, c) comparison with the Bird code simulation (20 Pa, 3000 sccm Ar, 120 sccm H_2, 40 A).

Measurements have been performed at a pressure of p_B = 20 Pa and with flow $\hat{\Phi}$ = 50 sccs argon and 4 % hydrogen admixture. The current in the source was 40 A and this leads to an exit source temperature of approximately $\hat{T}_s$ = 0.6 eV. The position of the shock front is then expected to be at z_M = 68 mm, whereas at half z_M the density starts to drop below the value outside the shock. The fluorescence has been measured at many points and in figure 2 several measured velocity profiles are shown for the positions 20, 50 and 80 mm, both on the axis and on a radial position of 20 mm. At z = 20 mm, still in the first expansion from the source, the axial profile shows perfectly the supersonic part with a velocity equal to 3100 m/s, in good agreement with $2c_0$, with c_0 = 1550 m/s the sonic velocity at the exit of the arc source with a temperature of T_s = 0.6 eV. At z = 20 mm, r = 20 mm already a second distribution is observed with zero velocity, not unexpected as it is at the edge of the barrel shock. At z=50 mm the scattered in distribution is already more important than the supersonic one at r = 20 mm, whereas it is just coming up at the axis. At z = 80 mm just beyond the calculated shock front position the second distribution is the most important at both radial positions. Hence the shock transition is diffuse, as expected in these rarefied conditions. The second slower distribution invades from the outside of the shock gradually to the axis and this process is complete at the position of the stationary shock front. Note that from figure 2 also the correspondence between axial and transverse profiles is clear: the ratios and relative values of the two distributions are the same for both ⊥ and || measurements. The radial off centre velocity component corresponds to a projected expansion velocity, as is clear from the r = 20 mm measurements for z = 20, 50 and 80 mm. In figure 3 the flow pattern is shown with the average velocity together with the very similar one found by the Bird DSMC code.

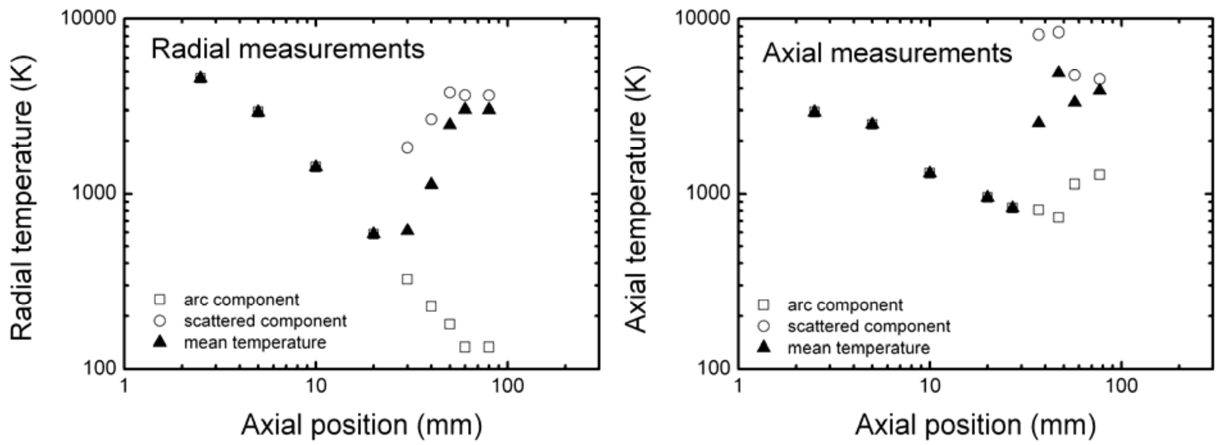

Figure 4. Temperatures of the two distributions as function of distance to the source. Note the difference between $T_{\perp}$ and $T_{//}$ starting at z = 20 mm for the supersonic component (open squares). The temperature of the scattered component (open circles) is similar to the temperature of the shock.

The temperatures deduced from the measurements are shown in figure 4. The temperatures of the supersonic component shows first the expected adiabatic decay with $(z_0/z)^{4/3}$; but then at z=20 mm the parallel temperature remains constant, whereas the transverse temperature keeps cooling adiabatically. It is the expected behavior if at z =20 mm the mean free path, $\lambda^{00}{}_{mfp}$, becomes equal to the gradient length, $L_{\nabla} = n/\nabla n$ [7]. It shows also that after the shock the cooling continues to 100 K.

From the measurements presented above it is clear that the supersonic distribution dominates the first part of the expansion, but that the influence of the scattered in component gradually becomes more important from the outside to the inside. This is clearly visible in figure 5 in which the density of the scattered component n_2 and next to it the ratio $n_1/(n_1 + n_2)$ is shown as contour plots. Gradually the scattered component takes over from the outside to the inside for rarefied conditions. It permits molecules from the outside to enter effectively the main plasma beam and it causes an effective mixing of molecules, injected or produced.

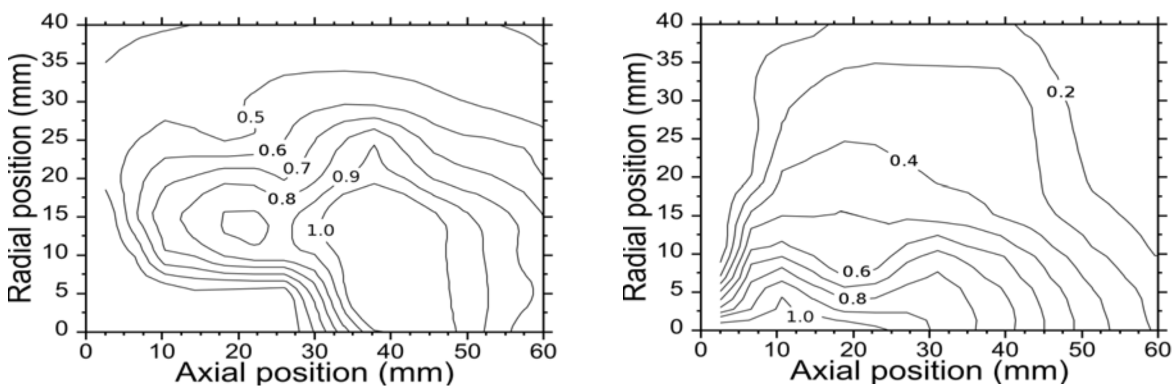

Figure 5. Contour plots of the density of the scattered component in arbitrary units (left) and of the ratio of the density of the expanding component to the total density (right).

A sign of such entrainment is also found in an experiment in which oxygen is injected in the background of an argon plasma. Here atomic oxygen was always present at the center axis of the expansion. The oxygen molecules are apparently invading the shock far before the shock front at z_M. In a later publication further details will be given with velocity distributions.

CONCLUSIONS

With diode laser directed either parallel or perpendicular to the expansion axis LIF has been performed to obtain detailed information on velocity distribution of metastable argon (and metastable oxygen) atoms. The measurements show first the expected expansion of a hot plasma with acceleration, density decay and adiabatic cooling. This continues up to the overexpanded region where first at the periphery and later also at the axis a second distribution arises which is warm and slower than the supersonic one. The effect, earlier called invasion, is a very effective way of mixing seeded in molecules with the main plasma beam from the source. The invasion causes first the average temperature and density to rise before the shock front. A condition for this to happen is that the local mean free path λ^{00}_{mfp} is of the same order as the size of the shock, $z_M/2$. This condition can be rewritten as an upper limit for the product of the flow and background pressure: $\hat{\Phi} p_b = 2.5 \cdot 10^4 \hat{T}_b^2 / \left(\sqrt{A_s \hat{T}_s} \hat{\sigma}_{-19}^2 \right)$; a condition which requires large and hot plasma flows and still low pressure and thus effective pumping.

Diode laser excited LIF proved to be a very effective way to measure in great detail the expansion process and gives velocity distributions in two directions, with which flow patterns can be constructed.

The measured flow patterns and measured quantities are in good agreement with predictions of the Bird DSMC code. A next step could be to obtain from such a code also the detailed velocity distributions and to compare these with the measured quantities.

ACKNOWLEDGEMENT

The authors greatly appreciate the skillful technical assistance of M.J.F. van de Sande, A.B.M. Hüsken, H.M.M. de Jong, and J. Janssen. Support from NWO in the framework of a Russian support program, of Euratom in a fusion related study, and of FOM in a TFF program is gratefully acknowledged. The authors thank Stephan Heil for his unpublished data on argon neutral density.

REFERENCES

[1] R. Campargue, *J. Phys. Chem*. **88**, 4466 (1984)
[2] D.C. Schram, S. Mazouffre, R. Engeln, and M.C.M. van de Sanden, *The Physics of Plasma Expansion*, in: R. Campargue, *Atomic and Molecular Beams*, Springer, New York (2001)
[3] G. Pham-Van-Diep, D. Erwin and E.P. Muntz, *Science* **245**, 624 (1989)
[4] H.M. Mott-Smith, *Phys. Rev.* **82**, 885 (1951)
[5] S. Mazouffre, P. Vankan, R. Engeln and D.C. Schram, *Phys. Rev. E* **64**, 066405 (2001)
[6] R. Campargue, *J. Chem. Phys. 52*, 1795 (1970);
[7] R. Engeln, S. Mazouffre, P. Vankan, D. C. Schram and N. Sadeghi, *Plasma Sources Sci. Technol.* **10**, 595 (2001)
[8] M.C.M. van de Sanden, G.M. Janssen, J.M. de Regt, D.C. Schram, J.A.M. van der Mullen and B. van der Sijde, *Rev. Sci. Instrum.* **63**, 3369 (1992)
[9] R.F.G. Meulenbroeks, A.J. van Beek, A.J.G. van Helvoort, M.C.M. van de Sanden and D.C. Schram, *Phys. Rev. E* **49**, 4397 (1994)
[10] S. Mazouffre, M.G.H. Boogaarts, I.S.J. Bakker, P. Vankan, R. Engeln and D.C. Schram, *Phys. Rev. E* **64**, 016411 (2001)
[11] G.A. Bird, *Rarefied Gas Dynamics*, Proc 24 Int. Symp., Monopoly (Bari), Italy, 541 (2004)
[12] W. Young, *Phys. Fluids* **18**, 1421 (1975)
[13] S.E. Selezneva, M.I. Boulos, M.C.M. van de Sanden, R. Engeln and D.C. Schram, *J. Phys. D: Appl. Phys*. **35**, 1362 (2002)
[14] P. Vankan, D.C. Schram, R. Engeln, *Plasma Sources Sci. Technol.* **14**, 744 (2005)
[15] A.J.M. Buuron, D.K. Otorbaev, M.C.M. van de Sanden and D.C. Schram, *Phys. Rev.E* **50**, 1383 (1994)
[16] M.J. de Graaf, R. Severens, R.P. Dahiya, M.C.M. van de Sanden and D.C. Schram, *Phys. Rev. E* **48**, 2098 (1993)